

Preparation and properties of a strong and durable composite superhydrophobic coating

F. F. Mao^a, Changquan Li^{a,*}, T. C. Mao^a, Z. Y. Xue^a, G. Q. Xu^a, A. Amirfazli^b

^a*School of Materials Engineering, Jiangsu University of Technology, Changzhou 213001, China.*

^b*Department of Mechanical Engineering, York University, Toronto ON M3J 1P3, Canada*

In this paper, from the perspective of improving the durability of superhydrophobic coatings, a strong and durable superhydrophobic coating was prepared by a simple spray method. The coating has good chemical stability and mechanical durability. After soaking in aqueous solution with pH value of 1 and 14 for 30 hours and 24 hours respectively, the contact angle is 139.8 ° and 143.5 ° respectively. After 90 times of abrasion, the contact angle is still 148 ° and the coating shows excellent self-cleaning and antifouling properties.

(Received August 1, 2022; Accepted November 21, 2022)

Keywords: Superhydrophobic, Sericite, Nano-ZnO, Chemical stability, Mechanical durability

1. Introduction

In recent years, inspired by "biomimicry", more and more researchers have begun to pay attention to superhydrophobic surfaces, such as self-cleaning^[1], anti-icing^[2], oil-water separation^[3], anti-fogging and freezing Frost^[4], antifouling^[5], drag reduction^[6] and other fields have been widely used, its unique superhydrophobicity also plays an important role in reducing the corrosion of metal materials in the atmosphere, ocean, soil, and even industrial environments. However, the microstructure of the surface of the superhydrophobic coating is fragile, and it is extremely difficult to recover after physical damage such as friction and extrusion, so that the coating loses the superhydrophobicity and limits the practical application of the superhydrophobic surface^[7]. Therefore, the development of a series of superhydrophobic surface coatings with comprehensive properties such as self-cleaning, anti-corrosion, and good mechanical stability and their construction technology is an important research direction today, with broad application prospects.

Superhydrophobic surface with a water contact angle (WCA) greater than 150° and a sliding hysteresis angle (SHA) below 10°. As long as there is a slight inclination, water droplets can slide off the surface without wetting the surface^[8, 9]. There are two key factors in the

* Corresponding author: cql6660607@163.com

construction of superhydrophobic surfaces: one is that the surface has a certain roughness, and the other is that the surface has a low surface energy^[10, 11]. In nature, the silt of lotus flowers and the sliding water droplets on lotus leaves are the result of the special structure of the surface^[12, 13]. Based on the above two key factors, scientists have explored a variety of methods to prepare superhydrophobic surfaces: dip coating, sol-gel method, hydrothermal method, surface etching method, electrospinning method, chemical vapor deposition, anodization, laser treatment method, etc.^[14-24]. Zhang et al.^[25] prepared a mixed superhydrophobic suspension of fluorine-free resin and hydrophobic SiO₂ nanoparticles with a particle size of about 10 nm. The superhydrophobic mixed suspension is sprayed on the surface of the substrate by a simple spraying method to obtain a superhydrophobic coating with high transparency and strong durability. The WCA of the coating is 160° and the sliding angle is less than 3°. Xiu et al.^[26] experimentally demonstrated that the superhydrophobic structure of the micro and nano scale hierarchical structures remained more intact after mechanical abrasion than the nano-scale superhydrophobic surface alone.

In this paper, epoxy, sericite and nano-ZnO were added to anhydrous ethanol in turn to disperse uniformly by blending method, and then the mixed solution is hydrophobically modified. Finally, the uniformly dispersed mixed solution is sprayed on the surface of aluminum sheet to obtain sericite@ZnO/epoxy (Ser@ZnO/EP) composite superhydrophobic coating. The effects of the mass ratio of sericite and nano-ZnO, the mass ratio of surface modifier and nanoparticles on the hydrophobicity of the coating were investigated. The chemical and mechanical durability properties of superhydrophobic coatings such as acid, alkali and salt corrosion resistance and abrasion resistance were studied.

2. Experimental

2.1. Materials

Epoxy (EP, E51) and 650 polyamide resin were purchased from Shanghai Mijiazhan Adhesive Products Co. Ltd. Octadecyltrimethoxysilane (ODTMS, 90%) was purchased from Shanghai McLean Biochemical Technology Co. Ltd. Sodium chloride (NaCl), sodium hydroxide (NaOH), hydrochloric acid (HCl), absolute ethanol, and ammonia water were all of analytical grade and were purchased from Sinopharm Chemical Reagent Co. Ltd. ZnO (30 nm) was purchased from Guangzhou Changyu Chemical Technology Co. Ltd. Sericite (Ser, 600 mesh) was purchased from Chuzhou Wanqiao Sericite Co. Ltd.

2.2. Preparation of superhydrophobic nanocomposite coatings

The aluminum sheet (5×6 cm) was sanded from two vertical directions with 240 sandpaper, and then washed in an ultrasonic cleaner with anhydrous ethanol and deionized water in a cycle to remove the remaining impurities on the surface of the aluminum sheet, and finally dried in a vacuum drying box for later use.

Add 2g EP, 80mL absolute ethanol, sericite and nano-ZnO (the total of sericite and nano-ZnO is 8g, weighed according to a certain proportion) into the beaker in turn. Ultrasonic vibration dispersion for 30min, and then magnetic stirring at 800r/min for 2h to obtain a uniformly dispersed mixed solution. Add 0.2g ODTMS to the mixed solution, stir magnetically for 2h. Finally, 2 g of 650 polyamide resin was added dropwise and stirred for 1 h to obtain a

uniformly dispersed mixed solution. The above obtained mixed solution is sprayed on the surface of the aluminum sheet by one-step spraying method (The diameter of the spray gun is 0.5mm, the distance between the nozzle and the surface of the aluminum sheet is 10-15cm, and the spraying speed is about 5cm/s under 0.5mPa with a Z-shape method for evenly spraying for 1min.), after curing at room temperature for 24 h, the Ser@ZnO/EP composite superhydrophobic coating was prepared. The preparation process is shown in Fig 1.

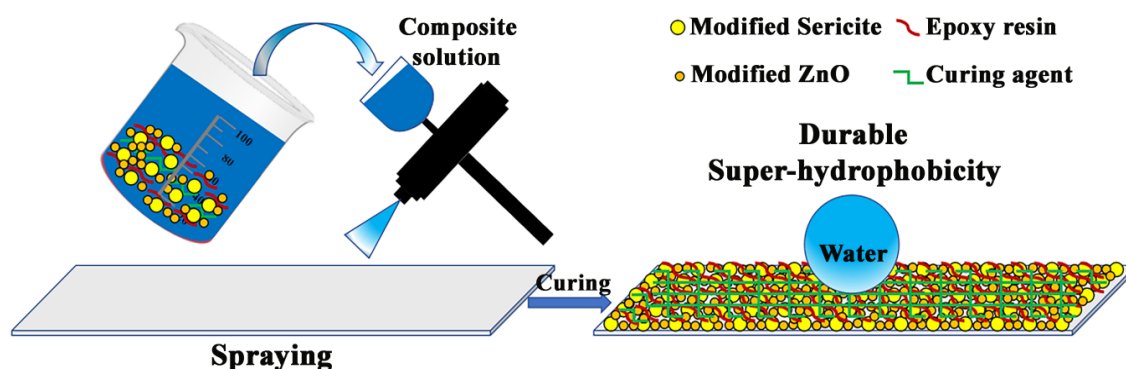


Fig. 1. Schematic illustration of the durable super-hydrophobic coating fabricated process.

2.3. Characterization and performance testing of samples

The hydrophobically modified nanoparticles were analyzed by Fourier transform infrared spectroscopy (FTIR, Nicolet iS5). The microstructure of the superhydrophobic composite coating was analyzed by scanning electron microscopy (SEM, FEI QUANTA FEG 400). The surface element analysis of the superhydrophobic composite coating was carried out by energy dispersive spectrometer (EDS, EDAX GENESIS). The wettability of the samples was measured by a contact angle meter (Krüss, DSA 30). The volume of the water droplet used was 10 μ L, and the test was repeated at 5 different positions of the sample, and the average value was taken as the test value.

Corrosion resistance test: Immerse the samples in aqueous solutions with pH values of 1, 3, 5, 7, 9, 11, 13 and NaCl (3.5wt%) aqueous solutions, take them out at regular intervals, wash them with water, and dry them, then test the wettability of the samples and record the surface wetting of the samples sexual changes.

Abrasion resistance test: Place the side of the aluminum sheet (3cm \times 2cm) sprayed with super-hydrophobic coating on 1000-mesh sandpaper, apply a load of 5.66kPa, corresponding to a weight of 100g, and push it in the horizontal direction at a speed of about 5cm/s, each time Push 10cm horizontally, and record the change of surface wettability of the sample every 10 times.

Coating binding force measurement: Coating adhesion is tested using cross hatch tests according to Standard (ISO 2409: 2007). Specifically, six parallel cuts were manually cut in two orthogonal directions using a cutter with six blades spaced 2 mm apart to form a lattice pattern on the coating. Apply tape over the lattice pattern cutouts and flatten the tape. Within 5 minutes of applying the tape, at an angle of 60 degrees, peel off the tape smoothly within 0.5 seconds to 1 second.

High temperature test: The samples were put into a muffle furnace, and the temperature was increased from 100 ° C to 300 ° C in an interval of 50 ° C for 2 hours. After the samples were cooled in the furnace, they were taken out to test their wettability.

Self-cleaning test: The iron oxide red pigment (30nm) was spread on the surface of the aluminum sheet and the sample through a 200-mesh wire mesh (the aluminum sheet and the sample were at a certain inclination angle to the horizontal plane), and observe how the water droplets roll and take away the red iron oxide pigment.

3. Results and discussion

3.1. Influencing factors of coating wettability

3.1.1. Influence of preparation process

There are two key factors in the construction of superhydrophobic surfaces: one is that the solid surface has a certain roughness; the other is that it has a low surface energy^[10-11]. In this paper, micro-nano rough structure is constructed by micro-scale sericite and nano-scale ZnO. The effect of the mass ratio of sericite and nano-ZnO on the hydrophobicity of the coating was explored. The test results of the contact angle and sliding angle are shown in Fig. 2(a). From Fig. 2(a), it can be seen that when sericite is used alone, the WCA is 149° and the sliding angle is 53°, and when nano-ZnO is used alone, the WCA is 157.9° and the sliding angle is 3°. When sericite is mixed with nano-ZnO, as the amount of nano-ZnO increases, the amount of sericite decreases, the contact angle increases, and the sliding angle decreases. When the mass ratio of sericite and nano-ZnO is 1:3, the hydrophobicity of the coating reaches the best, the WCA is 162.5°, and the sliding angle is 4.5°. This is because the mixed use of particles with different particle sizes can better build the micro-nano rough structure.

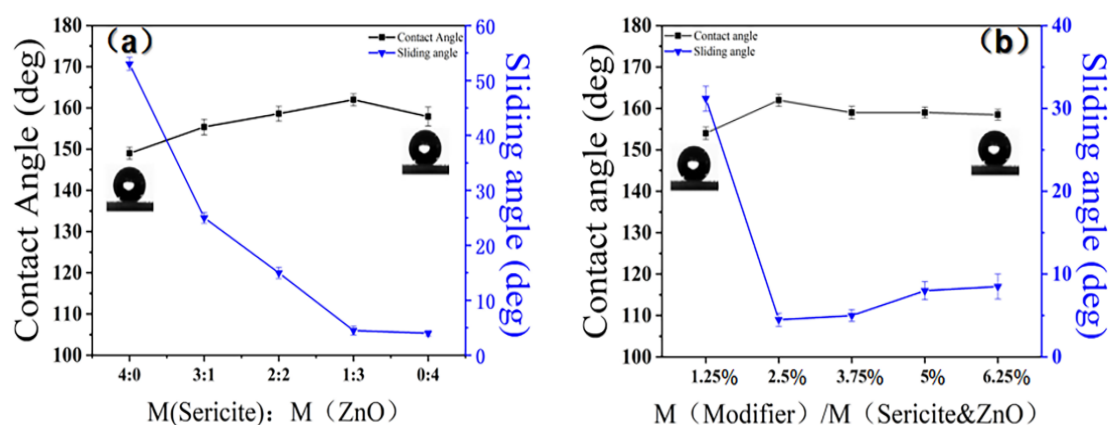


Fig. 2. The effect of the mass ratio of sericite and nano-ZnO on the hydrophobicity of the coating (a); the effect of the mass ratio of surface modifier and nanoparticles on the hydrophobicity of the coating (b).

Keeping the mass ratio of sericite and nano-ZnO at 1:3 unchanged, the effect of the mass ratio of surface modifier and nanoparticles on the hydrophobicity of the coating was explored. The test results of the contact angle and sliding angle are shown in Fig. 2(b). It can be seen from Figure 2(b) that when the dosage ratio of ODTMS and nanoparticles is 1.25%, the WCA is 154° and the sliding angle is 31.2° . Although the contact angle meets the superhydrophobicity requirement, due to the large sliding angle, The surface adhesion of the coating is large, resulting in a general hydrophobic effect of the coating. When the ODTMS content is 2.5%, the coating wetting performance reaches the best, the WCA is 162.5° , and the sliding angle is as low as 4.5° . Continuing to increase the content of ODTMS, the WCA and sliding angle of the coating remain basically stable, because the surface energy of the coating is very low to a certain extent and it is difficult to continue to decrease. Considering the economy and practical effect, the ODTMS content of 2.5% is the best.

3.1.2. Influence of surface chemical composition and morphology

The obtained Ser@ZnO/EP superhydrophobic coatings were characterized by SEM and EDS. From the low-magnification SEM image of Fig. 3(a), a dense coating with multi-scale structure is observed, consisting of micro-scale microspheres and pits. From the high-magnification SEM images of Fig. 3(b), (c), (d), it can be seen that the morphology contains many micro-nano papillae, which are formed by the aggregation of ZnO nanoparticles. The gaps between the microspheres and the pits of different scales can form a stable air layer, which is conducive to the construction of a solid-liquid-gas three-phase stable structure conforming to the Cassie-Baxter superhydrophobic model.

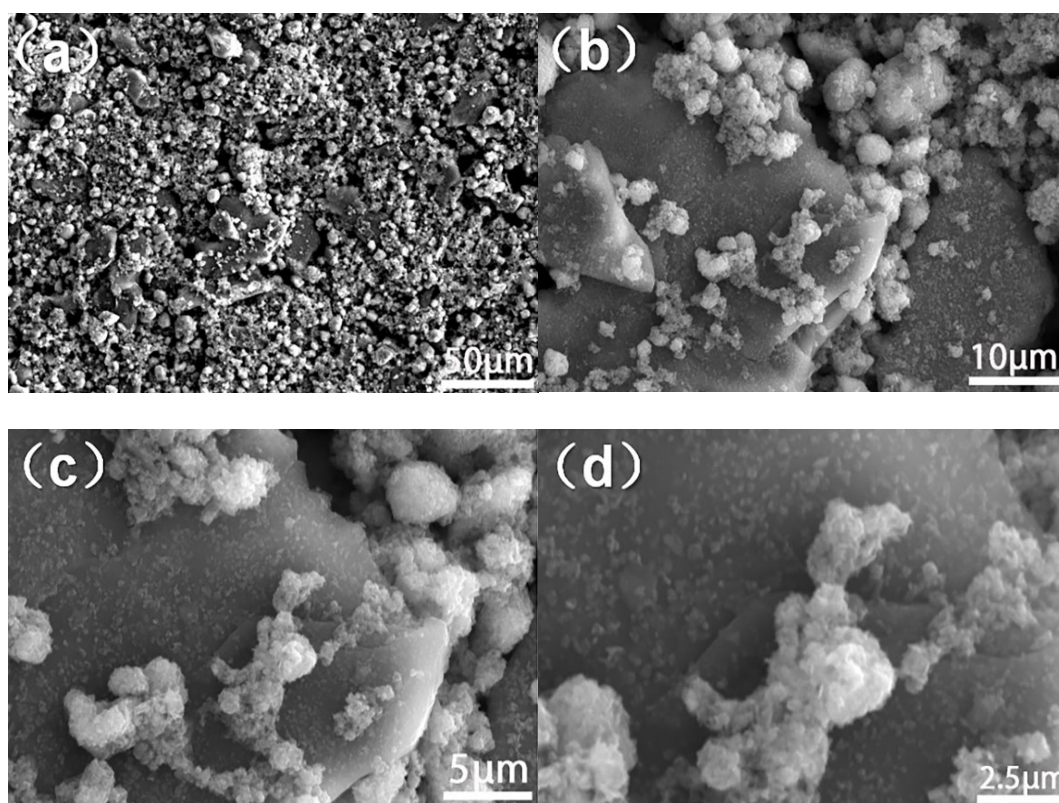


Fig. 3. SEM of the surface of aluminum sheet treated with superhydrophobic coating.

As shown in Fig. 4, the EDS spectrum shows that the characteristic elements of the coating include O, Zn, Si, Al and K, whose weight percentages (wt%) were 53.8%, 26.3%, 14.4%, 4.3% and 1.2%, respectively. It can be seen from Fig. 4 that the Zn element is uniformly distributed throughout the coating. The three elements of Si, Al and K are mainly provided by sericite, and some Si elements are provided by ODTMS. The distributions of the three elements Si, Al and K complement each other so that they are uniformly distributed throughout the coating.

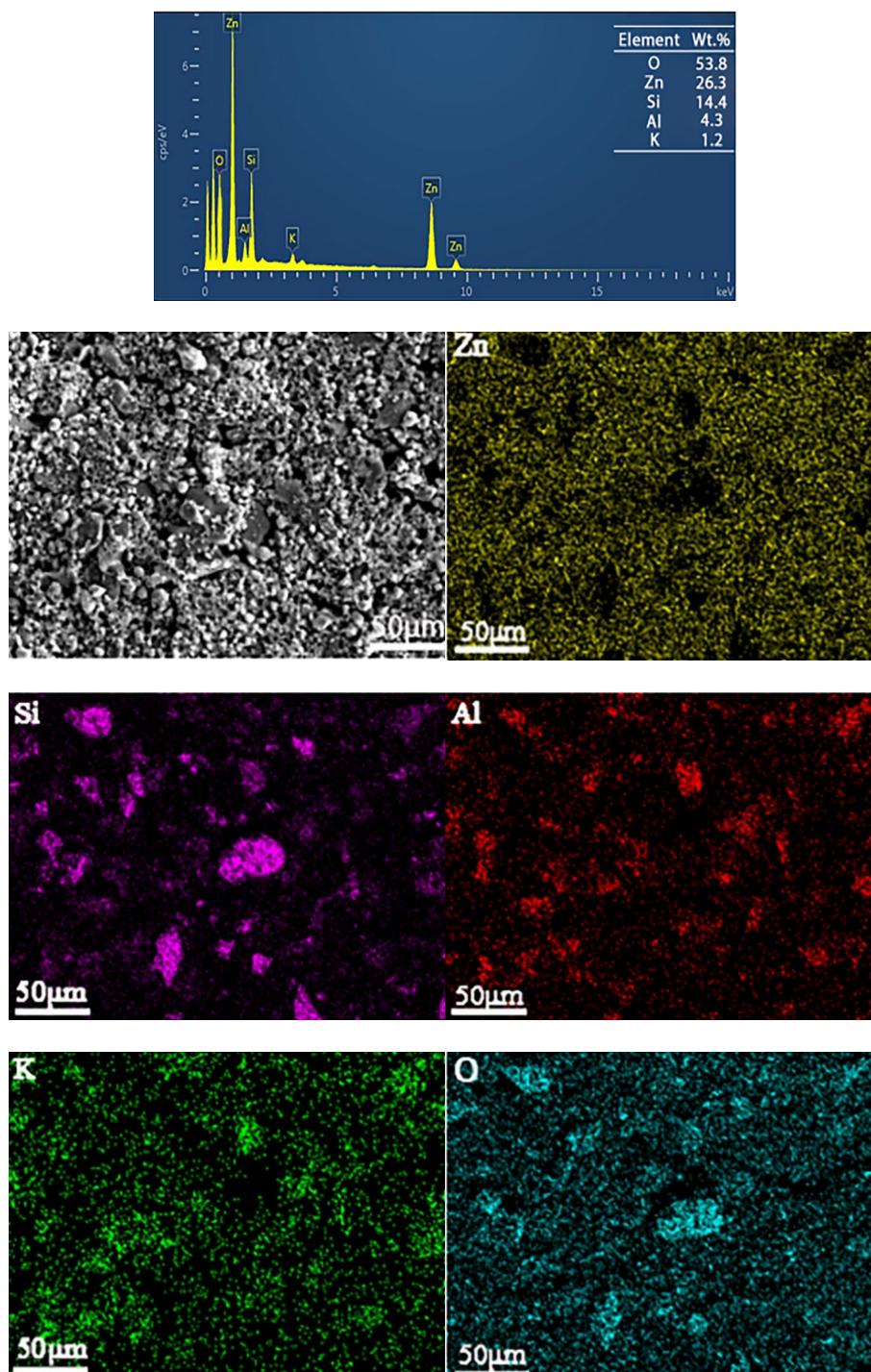


Fig. 4. Elemental composition and distribution of EDS.

The FTIR of sericite and nano-ZnO mixed modification is shown in Fig. 5(a). The strong absorption peak at 3370.56cm^{-1} in the spectral line is the stretching and bending vibration absorption peaks of hydroxyl or bridged hydroxyl, which is the adsorption of a large number of water molecules on the surface of SiO_2 and nano-ZnO, and the final dissociation of water molecules to form adsorbed hydroxyl^[27]. In Fig. 5(a), compared with the spectral lines a and c, 2917.96cm^{-1} is the stretching vibration peak of $-\text{CH}_3$ and $-\text{CH}_2$, which indicates that ODTMS was successfully grafted on the nanoparticles. The absorption peak at 1506.39cm^{-1} is the moisture contained in potassium bromide. The peak at 1468.38cm^{-1} is the vibration peak generated by $-\text{COOR}$ of ODTMS. 984.64cm^{-1} is the antisymmetric contraction vibration peak of Si-O-Si bond^[28]. 794.55cm^{-1} is the contraction vibration peak of Zn-O bond, which is formed due to the dehydration reaction of ODTMS with $-\text{OH}$ on the surface of SiO_2 and ZnO after hydrolysis to Si-OH^[29], as shown in Fig. 5(b).

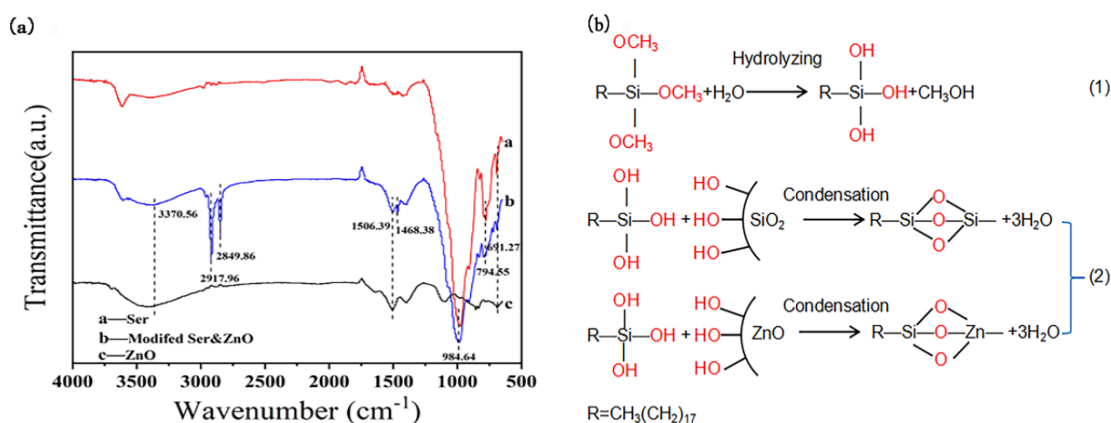


Fig. 5. Infrared spectra of different samples (a); possible reaction mechanism of ODTMS for nanoparticle modification (b).

3.2. Stability test of superhydrophobic coating

3.2.1. Corrosion resistance test

For practical applications, the durability of superhydrophobic coatings is a major consideration^[30-32]. Therefore, the stability of the samples was tested in aqueous solutions of different pH values and NaCl (3.5wt%) corrosive solution. The samples were taken out at intervals and washed with deionized water and then dried, and the changes in the wettability of the samples were recorded. As shown in Fig. 6.

It can be seen from Fig. 6(a) that with the increase of acidity and alkalinity, the contact angle decreases and the rolling angle increases, however, even after immersion in aqueous solutions of pH 1 and 13 for 24 h, the WCA still remains greater than 150° , but the sliding angle changes greatly. This is because a large number of acid-base ions invade the surface of the superhydrophobic coating and destroy the micro-nano structure on the surface of the superhydrophobic coating. The coatings remained superhydrophobic at pH 5-9, with WCAs higher than 150° and sliding angles lower than 10° . It can be seen from Fig. 6(c), (d) that the sample was immersed in an aqueous solution with a pH value of 1 for 30 hours, and the coating

WCA was 139.8° ; the immersion time in an aqueous solution with a pH value of 14 was 24 hours. , the coating WCA is 143.5° . And the coating peeled off a little. It shows that the sample has good stability in acid and alkali.

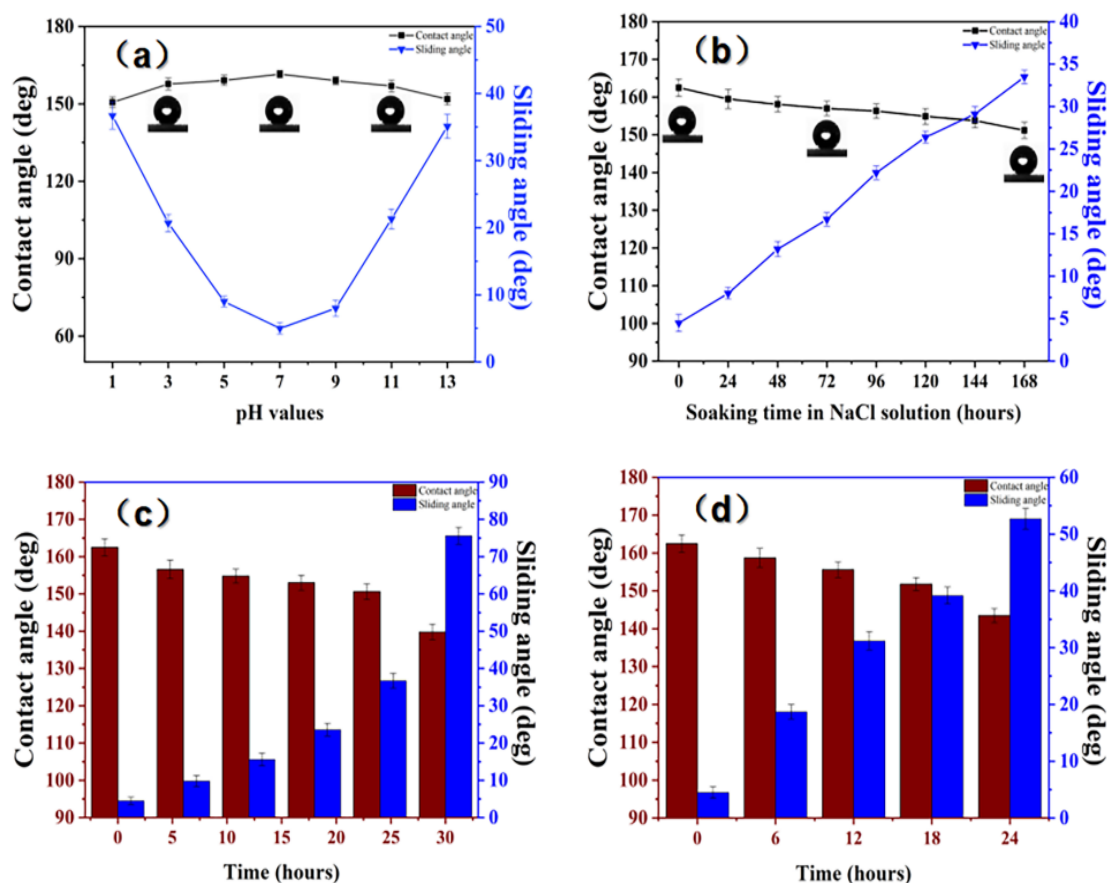


Fig. 6. The wettability relationship diagram of the sample after soaking in different pH solutions for 24h (a); the wettability relationship diagram of the sample soaking in NaCl (3.5wt%) solution for different time (b); the sample soaking in an aqueous solution with pH value of 1 The wettability graph (c) of the sample at different times in the water; the wettability graph of the sample immersed in an aqueous solution with a pH value of 14 at different times (d).

It can be seen from Fig. 6(b) that with the increase of the immersion time of the samples in the NaCl etching solution, the WCA of the samples gradually decreases, and the sliding angle gradually increases. After soaking for 168 hours, the WCA of the sample remains above 150° , the sliding angle increases to 33.5° , and the sample still maintains good hydrophobicity. It shows that the sample has good stability in NaCl etching solution.

The reason why the sample has good corrosion resistance is because the surface of the superhydrophobic coating has a low surface energy and has a strong repellency to liquids. At the same time, the micro-nano structure can form a stable air layer, and these air layers are effective. The immersion of corrosive media is prevented. The synergistic effect of the two reduces the contact between the corrosive medium and the coating, thereby enhancing the corrosion resistance of the sample. In addition, sericite itself also has excellent corrosion resistance, which

can effectively protect the coating from damage, further enhancing the corrosion resistance of the samples^[33,34].

3.2.2. Abrasion resistance test

In practical applications, superhydrophobic surfaces are often exposed to various complex and harsh environments, and over time, due to the destruction of various mechanical external forces, they will lose their superhydrophobicity. Fig. 7(a) is the technical model of the sandpaper wear test, and Fig. 7(b) is the relationship between the number of frictions and the wettability of the sample.

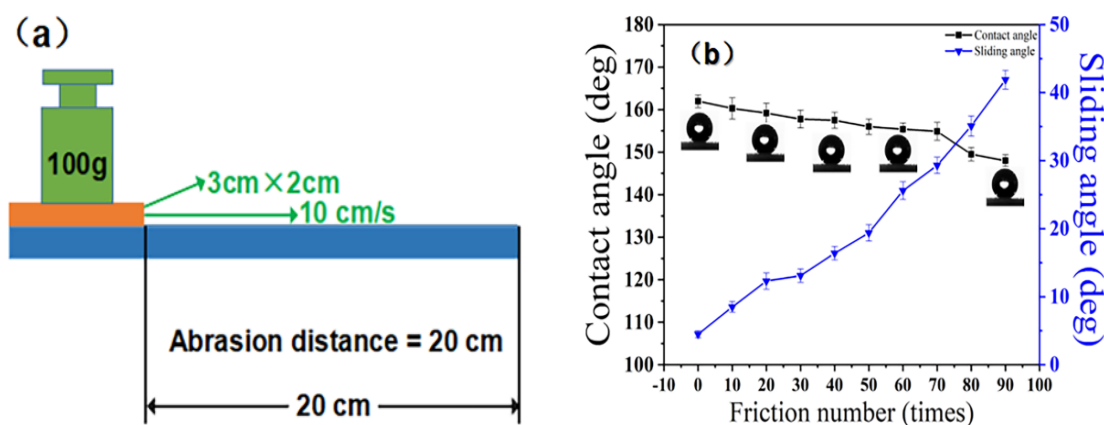


Fig. 7. Schematic diagram of (a) Abrasion test; relationship between friction times and wettability of samples (b).

It can be seen from Fig. 7(b) that the contact angle of the coating gradually decreases with the increase of the number of abrasions. When the number of abrasions reaches 70, the WCA is 154.9°, and the coating still has a superhydrophobic effect. When the number of abrasions exceeds 90 times, the coating loses superhydrophobicity, the WCA is still 148°, and the coating still has good hydrophobicity. This is because the micron-sized sericite has good abrasion resistance, and its existence effectively protects the nanoparticles from being damaged. At the same time, the EP firmly adheres the filled micro-nanoparticles to the surface of the aluminum sheet. The combined effect of the two promotes the coating to have better abrasion resistance.

3.2.3. Coating binding force measurement

Only when the superhydrophobic coating has a good bonding force with the substrate can it have broad application prospects in real life. Referring to the international standard ISO2409-2013, the adhesion of the coating to the substrate was evaluated by the tape peel test, as shown in Fig. 8. It can be seen from Fig. 8 (b1) and (d1) that the cutting edge is completely smooth without any mesh falling off. Compared with the international standard in Table 1, it can be determined that the binding force of the superhydrophobic coating reaches grade 0 (the highest grade). It shows that the superhydrophobic coating has excellent bonding force with the substrate.

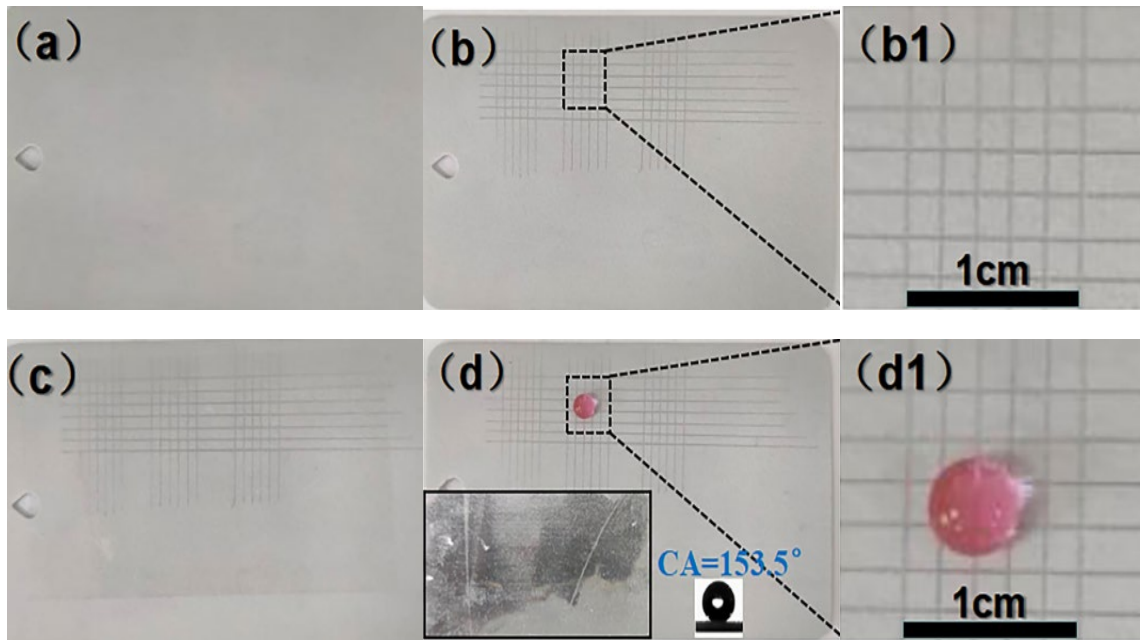


Fig. 8. Bonding force measurement of the superhydrophobic coating using cross hatch tests. (a) Appearance of the initial coating; (b) Construction of a cross pattern on the coated surface; (b1) Enlarged image of the crossed lines; (c) Tape on the intersection surface; (d) After removing the tape, a small amount of The powder adheres to the tape. (d1) Magnified image of the tested surface.

Table 1. Classification of experimental results with reference to international standards.

Grade	Illustration	Surface appearance of criss-cross cut areas that have fallen off (Take six parallel cutting lines as an example)
0	The cutting edge is completely smooth, and there is no falling off.	—
1	A little coating peeled off at the cut intersection. The cross-cut area should not be affected by more than 5%.	
2	Coating peeling off cut edges and/or intersections. The affected cut area is greater than 5% but less than 15%.	

3.2.4. High temperature test

The surface wettability of the Ser@ZnO/EP superhydrophobic coatings after being kept at different temperatures for 2 h was observed, and the results are shown in Fig. 9. As the temperature gradually increased, the color of the sample began to change. When the sample was kept at 300 °C for 2 h, the color of the coating changed to dark brown. However, in the entire temperature range of 100-300 °C, the WCA of the samples are all above 150°, and the sliding angles are all below 10°, indicating that the coating has good thermal stability.

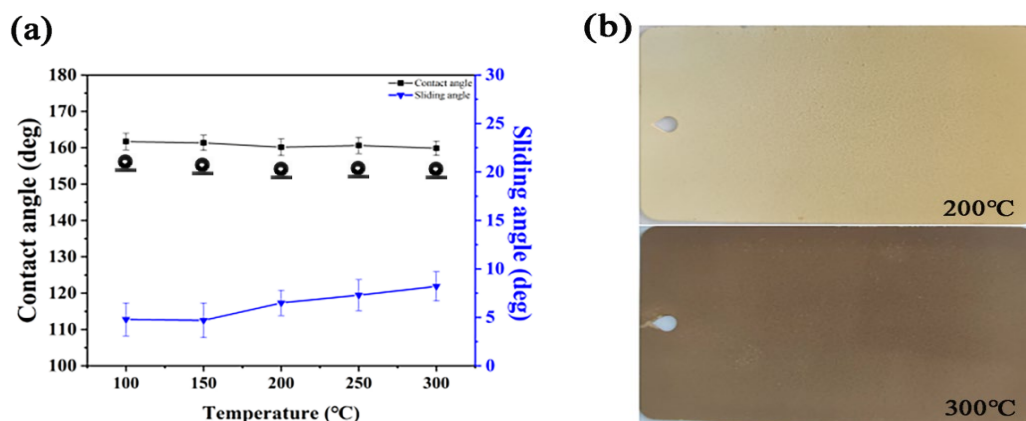


Fig. 9. Changes in wettability of samples after being incubated at different temperatures for 2 h(a); Changes in the surface of the sample after incubation at different temperatures (b).

3.3. Self-cleaning and antifouling properties

Sprinkle 0.1 g of iron oxide red pigment on the surface of aluminum sheet, ordinary coating and super-hydrophobic coating respectively through a 200-mesh copper mesh, place the samples at a certain inclination angle, and place the water droplets at the upper end of the sample about 1cm away from the surface of the sample through a dropper. It drips slowly and continuously, as shown in Fig. 10. It can be seen from Fig. 10 (a1-a2) that when the water droplets drip from the top of the aluminum sheet to the surface of the aluminum sheet in turn, the water droplets slowly slide from the surface of the aluminum sheet under the action of gravity and meet the iron oxide red pigment. The red pigment is absorbed, and the remaining water continues to slide down under the action of gravity, which can only take away a little iron oxide red pigment. It can be seen from Fig. 10 (b1-b2) that when the water droplets fall on the surface of the ordinary coating, the cleaning effect is no different from that of the water droplets on the surface of the aluminum sheet, and self-cleaning cannot be achieved. It can be seen from Fig. 10 (c1-c2) that when the water droplets successively drop onto the surface sprayed with the superhydrophobic coating, the bouncing and rolling water droplets adsorb the iron oxide red pigment and take it away without leaving any traces, indicating that the composite coating has excellent self-cleaning performance.

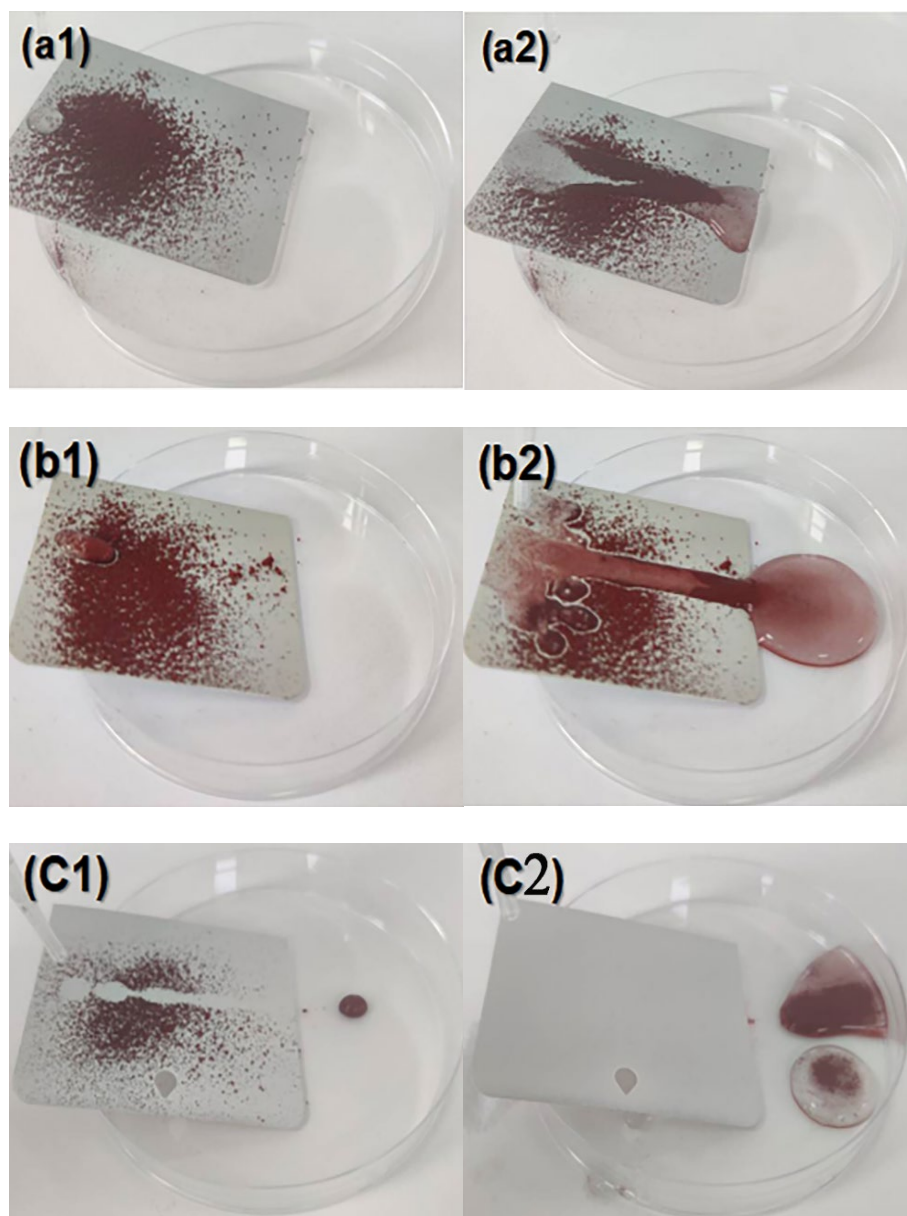


Fig. 10. Self-cleaning performance of aluminum sheet (a1-a2); ordinary coating (b1-b2) and superhydrophobic coating (c1-c2).

To test the antifouling properties of the coatings, aluminum flakes and aluminum flakes sprayed with a superhydrophobic coating were immersed in a methylene blue solution. Due to the hydrophilicity, the methylene blue solution was immediately adsorbed on the surface of the aluminum sheet, as shown in Fig. 11(a1-a4). However, the aluminum flakes sprayed with the superhydrophobic coating remained clean after immersion in the solution without any solution adsorbed on the surface, as shown in Fig. 11(b1-b4). The air layer trapped between the water and the textured surface effectively prevents the liquid from wetting and fouling the surface and thus showing excellent non-wetting performance^[35].

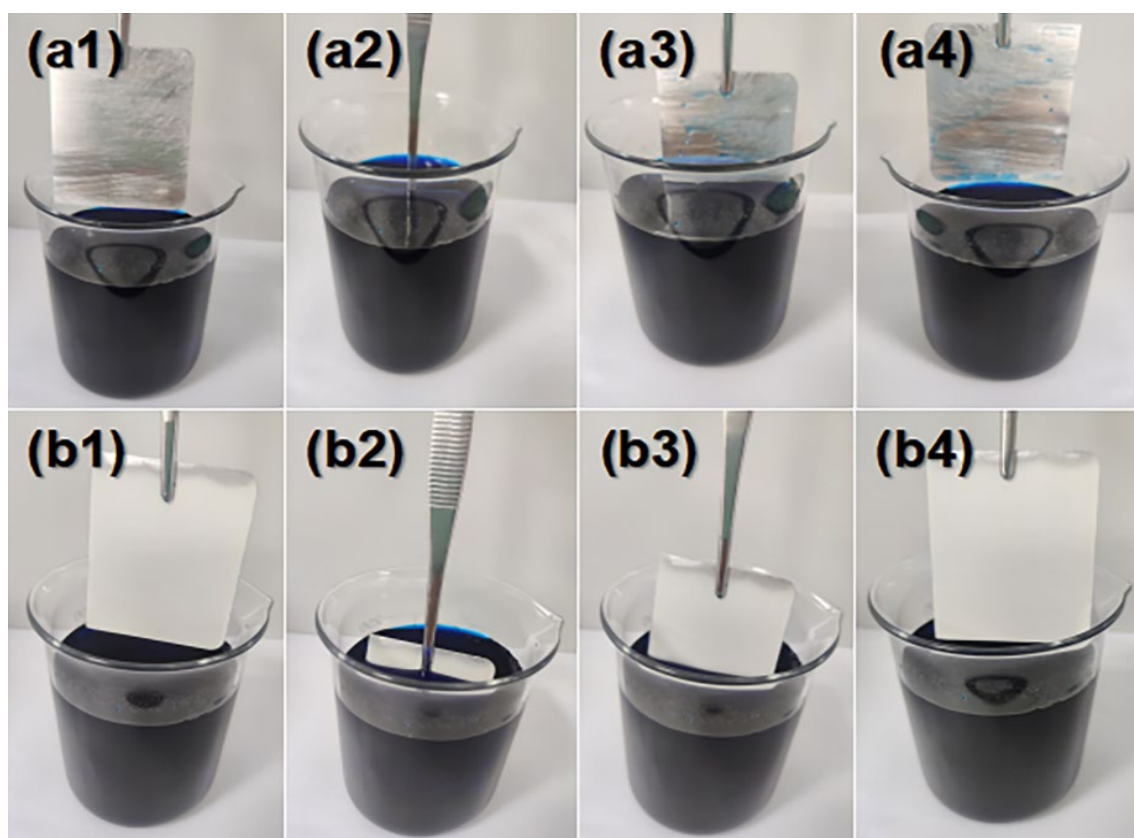


Fig. 11. Antifouling process of untreated aluminum flakes (a1-a4) and aluminum flakes treated with superhydrophobic coating (b1-b4).

4. Conclusions

In summary, a strong and wear-resistant superhydrophobic coating of Ser@ZnO/EP was prepared on the surface of aluminum sheet by a simple spraying method. Through the research on the influence of the mass ratio of sericite and nano-ZnO, the mass ratio of surface modifier and nanoparticles on the hydrophobicity of the coating, it is shown that the mass ratio of sericite to nano-ZnO was 1:3, and the mass ratio of surface modifier to nanoparticles was 2.5%. The prepared superhydrophobic coating had the best hydrophobicity, with a WCA of 162.5° and a sliding angle of 4.5° . The WCA of the prepared coatings were 139.8° and 143.5° after immersion in strong acid and strong alkaline aqueous solutions for 30 hours and 24 hours, respectively. After immersion in NaCl corrosive solution for 168 h, the WCA was 151.2° , and the coating still had good hydrophobicity, indicating that the coating had good corrosion resistance. At the same time, the coating has good adhesion performance and wear resistance, and the coating bonding force measurement reaches grade 0 (the highest grade); the surface WCA of the coating is 148° after 90 abrasion experiments. The superhydrophobic coating also displayed excellent self-cleaning and anti-fouling properties.

Acknowledgements

This work was supported by National Natural Science Foundation of China (52073127) and Changzhou Sci & Tech Program (CM20193004).

References

- [1] A. Cholewinski, J. Trinidad, B. McDonald, et al., Surface and Coatings Technology, 254 (2014) 230-237; <https://doi.org/10.1016/j.surfcoat.2014.06.020>
- [2] T. Rezayi, M.H. Entezari, Surface and Coatings Technology, 276 (2015) 557-564; <https://doi.org/10.1016/j.surfcoat.2015.06.015>
- [3] Y. Li, S. Chen, M. Wu, J. Sun, Adv. Mater. 26 (2014) 3344-3348; <https://doi.org/10.1002/adma.201306136>
- [4] C. Zhu, S. Liu, Y. Shen, J. Tao, G. Wang, L. Pan, Surf. Coat. Technol. 309 (2017) 703-708; <https://doi.org/10.1016/j.surfcoat.2016.10.098>
- [5] Y. Lu, S. Sathasivam, J. Song, F. Chen, W. Xu, C.J. Carmalt, I.P. Parkin, J. Mater. Chem. A 2 (2014) 11628-11634; <https://doi.org/10.1039/C4TA02181A>
- [6] Z. Sun, T. Liao, K. Liu, L. Jiang, J.H. Kim, S.X. Dou, Small 10 (2014) 3001-3006; <https://doi.org/10.1002/sml.201400516>
- [7] Zhang F, Chen S, Dong L, et al. Applied Surface Science, 2011, 257(7):2587-2591; <https://doi.org/10.1016/j.apsusc.2010.10.027>
- [8] A. Cholewinski, J. Trinidad, B. McDonald, et al., Surface and Coatings Technology, 254 (2014) 230-237; <https://doi.org/10.1016/j.surfcoat.2014.06.020>
- [9] T. Rezayi, M.H. Entezari, Surface and Coatings Technology, 276 (2015) 557-564; <https://doi.org/10.1016/j.surfcoat.2015.06.015>
- [10] Zhou H, Wang H, Niu H, et al., Advanced Materials, 2012, 24(18):2409-2412; <https://doi.org/10.1002/adma.201200184>
- [11] Lin, Feng, Zhongyi, et al., Angewandte Chemie International Edition, 2004; <https://doi.org/10.1002/anie.200353381>
- [12] Hsu C P, Chang L Y, Chiu C W, et al., Acs Applied Materials @ Interfaces, 2013, 5(3):538-545; <https://doi.org/10.1021/am400132p>
- [13] Accardo A, Gentile F, Mecarini F, et al., Langmuir the Acs Journal of Surfaces @ Colloids, 2010, 26(18):15057-64; <https://doi.org/10.1021/la102958w>
- [14] X. Gao, X. Wang, X. Ouyang, C. Wen, Sci. Rep. 6 (2016) 27207; <https://doi.org/10.1038/srep27207>
- [15] N. Mittal, D. Deva, R. Kumar, A. Sharma, Carbon 93 (2015) 492-501; <https://doi.org/10.1016/j.carbon.2015.05.086>
- [16] Bhushan B, Jung Y C, Niemietz A, et al., Langmuir the Acs Journal of Surfaces @ Colloids, 2009, 25(3):1659-66; <https://doi.org/10.1021/la802491k>
- [17] Li Q, Yan Y, Yu M, et al., Applied Surface Science, 2016, 367(Mar.30):101-108; <https://doi.org/10.1016/j.apsusc.2016.01.155>
- [18] Coclite A M, Shi Y, Gleason K K., Physics Procedia, 2013, 46(18):56-61;

<https://doi.org/10.1016/j.phpro.2013.07.045>

[19] Li D W, Wang H Y, Liu Y, et al., Chemical Engineering Journal, 2019, 367:169-179;

<https://doi.org/10.1016/j.ccej.2019.02.093>

[20] Li C, Sun Y, Cheng M, et al., The Chemical Engineering Journal, 2017:S1385894717316649;

<https://doi.org/10.1016/j.ccej.2017.09.165>

[21] Hosseinzadeh K, Ganji D D, Ommi F., Journal of Molecular Liquids, 2020, 315:113748;

<https://doi.org/10.1016/j.molliq.2020.113748>

[22] Wang, Jinfeng, Peng, Journal of Materials Chemistry A Materials for Energy @

Sustainability, 2016; <https://doi.org/10.1039/C6TA01082B>

[23] D. Zhang, L. Li, Y. Wu, W. Sun, J. Wang, H. Sun, Colloids Surf. A-Physicochem. Eng. Asp.

552 (2018) 32-38; <https://doi.org/10.1016/j.colsurfa.2018.05.006>

[24] J. Yong, Q. Yang, C. Guo, F. Chen, X. Hou, RSC Adv. 9 (2019) 12470-12495;

<https://doi.org/10.1039/C8RA10673H>

[25] Zhang C, Kalulu M, Sun S, et al., Colloids & Surfaces A Physicochemical & Engineering

Aspects, 2019, 570: 147-155; <https://doi.org/10.1016/j.colsurfa.2019.03.015>

[26] Qin L, Chu Y, Zhou X, et al., ACS Applied Materials & Interfaces, 2019, 11(32):

29388-29395; <https://doi.org/10.1021/acsami.9b07563>

[27] BingBing X U, Yue-Wen H, Bin W., Fine Chemicals, 2019.

[28] Ou J , Wang F , Li W , et al., Progress in Organic Coatings, 2020, 146:105700;

<https://doi.org/10.1016/j.porgcoat.2020.105700>

[29] Wei X L, Li N, Yi W J, et al., Surface @ Coatings Technology, 2017, 325;

<https://doi.org/10.1016/j.surfcoat.2017.06.004>

[30] Y.H. Xiu, Y. Liu, D.W. Hess, C.P. Wong, Nanotechnology 21 (2010) 155705;

<https://doi.org/10.1088/0957-4484/21/15/155705>

[31] T. Verho, C. Bower, P. Andrew, S. Franssila, O. Ikkala, R.H.A. Ras, Adv. Mater. 23 (2011)

673-678; <https://doi.org/10.1002/adma.201003129>

[32] L. Ionov, A. Synytska, Phys. Chem. Chem. Phys. 14 (2012) 10497-10502;

<https://doi.org/10.1039/c2cp41377a>

[33] D.H.K. Reddy, S. Lee, J. Kim, World Appl. Sci. J. 27 (2013) 1514-1523.

[34] J.O. Kim, S.M. Lee, C. Jeon, Chem. Eng. Res. Des. 92 (2014) 368-374;

<https://doi.org/10.1016/j.cherd.2013.07.020>

[35] X. Kong, J. Zhang, Q. Xuan, J. Lu, J. Feng, Langmuir 34 (28) (2018) 8294-8301;

<https://doi.org/10.1021/acs.langmuir.8b01423>